Extended Abstracts of the 18th (1986 International) Conference on Solid State Devices and Materials, Tokyo, 1986, pp. 339-342

Ballistic Transport of Quasi-Two-Dimensional Electron Gas at AlGaAs/GaAs Interface

K. Yokoyama, M. Tomizawa and A. Yoshii

NTT Electrical Communications Laboratories

3-1 Morinosato Wakamiya
Atsugi, Kanagawa 243-01, Japan

Ballistic transport of quasi-two-dimensional electron gas (Q2DEG) at an AlGaAs/GaAs heterointerface is confirmed using a Monte Carlo method. The model includes accurate physical descriptions, such as electronic states of the Q2DEG and corresponding two-dimensional scatterings for each subband. Ballistic transport is expected under low lattice temperatures, because the electrons are accelerated without undergoing polar optical phonon emission. It is concluded that this effect is advantageous for realizing ultra-high speed devices.

I. INTRODUCTION

For application to ultra-high speed transistors, such as HEMTs (High Electron Mobility Transistors)[1], much attention has been focused on AlGaAs/GaAs modulation doped heterostructures. In the AlGaAs/GaAs system, the free electrons are transferred to the high-purity GaAs layer where they populate a narrow potential well and form a quasi-two-dimensional electron gas (Q2DEG). Since the electrons are spatially separated from the ionized donors, they exhibit a high-electron mobility, as pointed out by Dingle *et al.*[2]. This is one of the most important features of HEMTs.

Deeper theoretical understanding of Q2DEG transport is needed to design an optimum device structure. The dominant lattice scattering[3]-[5] and impurity scattering[6],[7] for electrons in heterolayers have been extensively investigated. For simplicity, many authors have used square-well[4],[5] or triangular-well[8] potentials to discuss the electron mobility. Only electron mobility (steady state) values are discussed in the above cited publications by using a relaxation time which is closely related to the inverse of the scattering rates. On the other hand, precise calculation of electron properties for the Q2DEG including multisubband conduction have been reported based upon ensemble Monte Carlo[9],[10]. The outline of the simulation is briefly reviewed in Section II.

In this paper, the application of the simulator to modulation doped heterostructures having different spacer thicknesses is described. In Section III, ballistic transport for the Q2DEG is discussed through the drift velocity responses. The discussion also includes the dominant two-dimensional scattering rates to clarify the ballistic transport. Finally, the advantages of the excellent transport features in low fields, which promote high speed operation, are described.

II. OUTLINE OF SIMULATION

One-dimensional cross section under the gate for HEMT (perpendicular to the heterointerface; see Fig. 1) is used in the present study. The electronic states of the AlGaAs/GaAs single quantum well are calculated self-consistently by taking the five lowest subbands into account. Table 1 shows the obtained energy eigenvalues and the Fermi energy. The calculated potential and electron density distribution along with the energy levels (E_m for the m-th subband) at lattice temperature (T_l) of 77 K are indicated in Fig. 1. For the conditions shown in Fig. 1, subband separation E_2-E_1 is 29.2 meV, which is considerably greater than $k_B T_l$. Therefore, the size quantization effects in the Γ-valley of the GaAs layer (region I of Fig. 1) are

Table 1 Binding Energies and Electron Population

mth	77 K		300 K	
Subband	E_m (meV)	Popul. (%)	E_m (meV)	Popul. (%)
1	47.8	94.6	50.3	65.7
2	77.0	5.0	86.6	19.0
3	94.5	0.4	108.9	8.3
4	108.7	...	125.6	4.4
5	121.1	...	139.5	2.6
E_F	64.1	...	35.9	...

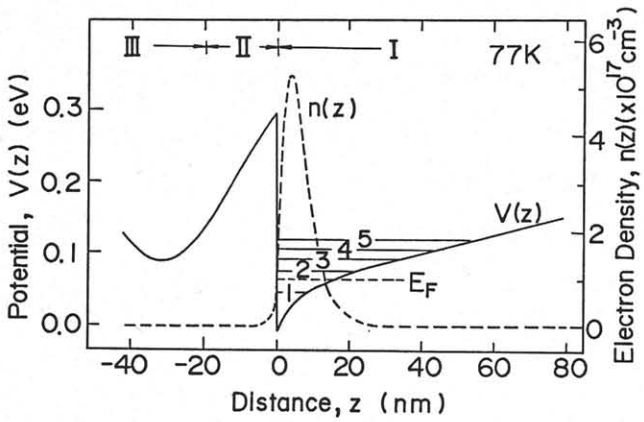

Fig. 1 Calculated effective potential and electron density distribution at 77 K. The numbers in the figure indicate the quantized energy levels of the five lowest subbands. The following parameters are assumed in this calculation: 5×10^{11} cm^{-2} electrons in channel (N_s), an acceptor doping of 1×10^{15} cm^{-3} in the GaAs layer (Layer I), a modulation doping of 5×10^{17} cm^{-3} of $Al_{0.3}Ga_{0.7}As$ (Layer III) and a non-intentionally doped $Al_{0.3}Ga_{0.7}As$ spacer (Layer II).

accounted for. The electrons in the L- and X-valleys of the GaAs layer and those in the AlGaAs layer are treated as three-dimensional.

Numerically obtained energy levels and envelop functions (F_m for the m-th subband) have been used to calculate the major two-dimensional scattering rates in each subband. The calculated phonon scattering rates for the first subband at T_l = 77 K corresponding to Fig. 1 and Table 1 are summarized in Fig. 2. The dashed lines indicate the three dimensional polar optical phonon scattering rates[11]. The detailed discussion of this figure has been described in Ref.[9].

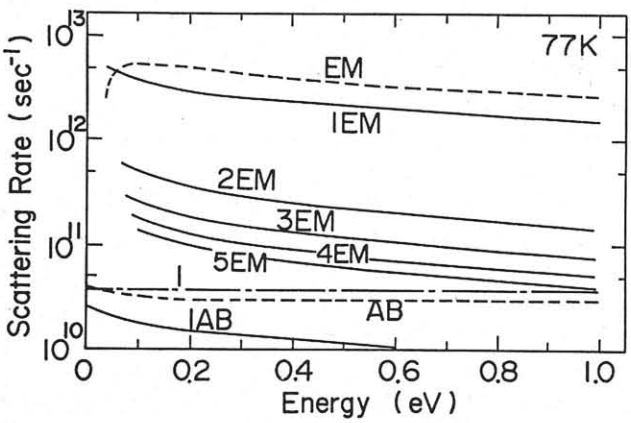

Fig. 2 Phonon scattering rates versus energy for the first subband at 77 K. The numbers in the figure show the final subband. Solid and dashed lines shows the rates for two- and three-dimensional polar optical phonon scattering, respectively. EM and AB stand for emission and absorption, respectively. The dashed-dotted line indicates the rates for acoustic phonon scattering.

The screening effects due to the electrons in the five lowest subbands are taken into account for ionized impurity scattering to obtain the Fourier transformed Coulomb potential ($\varphi(Q,z)$) used to calculate the matrix element. The calculated screening constants for the three lowest subbands are 1.81×10^6, 2.45×10^5, and 1.99×10^4 cm^{-1} under the conditions shown in Fig. 1. The matrix element for the electron-impurity interaction is obtained by

$$|M_{mn}(Q)|^2 = \int M_{mn}^2(z_0)N_I(z_0)dz_0, \qquad (1)$$

with

$$M_{mn}(z_0) = \int e\varphi(Q,z)F_m(z)F_n(z)dz, \qquad (2)$$

where $N_I(z_0)$ represents the impurity concentration at $z = z_0$. In the integration of Eq. (1), contributions due to remote impurity scattering ($z_0 < 0$) and background impurity scattering ($z_0 > 0$) are considered.

In the Monte Carlo calculation, the trajectories of many electrons (10,000 particles in the present study) are monitored simultaneously under uniform field (F) conditions along the heterointerface to study the transient bahavior. The transport properties are calculated as an ensemble average of the assumed particles. For an electron in each subband of the GaAs layer, 16 possible scattering mechanisms are taken into account. These include 10 polar optical phonon scattering processes for emission and absorption (intersubband and intrasubband transitions), intrasubband acoustic phonon transitions, intrasubband impurity scattering, and intervalley scattering to L- and X-valleys.

III. RESULTS AND DISCUSSION

The simulator is applied to the modulation doped heterostructures having different spacer thicknesses (d) (region II in Fig. 1). As shown in Table 1, most of the electrons populate in the lowest subband. Then, scattering rates in the lowest subband are very important. For ionized impurity scattering, the intersubband scattering rates are smaller than the intrasubband's[9]. By increasing thickness d, the scattering rates are suppressed, as shown in Fig. 3, due to the reduction of remote impurity scatterings. Therefore, mobility is enhanced with increases in spacer thickness. This effect has been proven using a relaxation time without applying the fields at low temperatures[12].

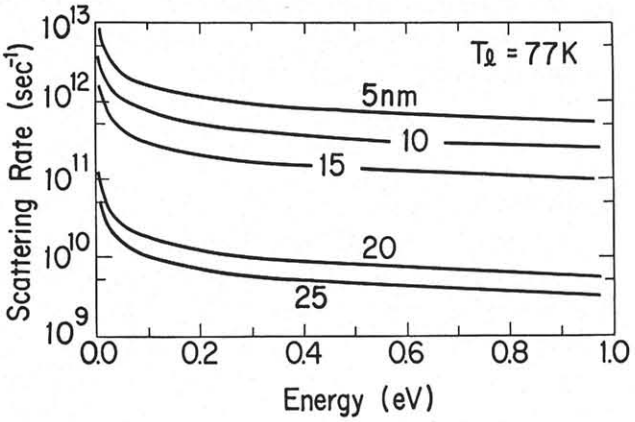

Fig. 3 Intrasubband ionized impurity scattering rates for different spacer thicknesses in the lowest subband at 77 K.

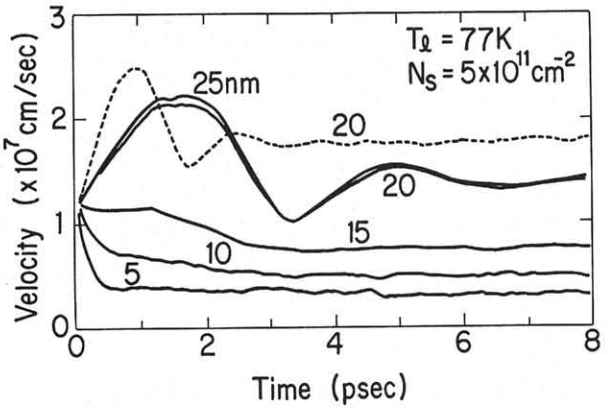

Fig. 4 Transient velocity characteristics for different spacer thicknesses. Solid lines show the responses at F = 500 V/cm. Dashed line indicates the results at F = 1 kV/cm.

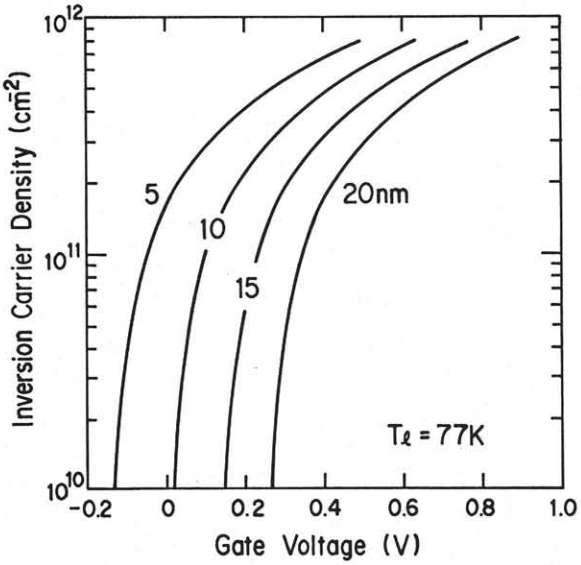

Fig. 5 Inversion carrier density versus gate voltage. Schottky barrier height of 0.8 eV is assumed.

Our calculated transient responses also concur with the above steady state results, as shown in Fig. 4. The calculated mobility is 2.5×10^4 cm^2/Vsec for d = 20 nm at F = 500 V/cm. Figure 4 also shows that a 20 nm spacer is sufficient to eliminate the remote ionized impurity scattering.

On the other hand, induced inversion carrier density (N_s) decreases with increases in the spacer thickness in the modulation doped structure, as shown in Fig. 5. Similar results are reported in Ref. [13]. In addition, decrease in N_s value results in reduction of the screening effect. From the viewpoint of transistor parameters, the thin AlGaAs layer (sum of regions II and III) enhances the transconductance (g_m) values[14]. Then, to obtain high g_m values, the design principle for HEMT surface AlGaAs thicknesses is the same as that for MOSFET oxide thicknesses. After extending the present work to discuss transistor parameters, optimum spacer thickness can be determined by the above tradeoffs.

Moreover, the present transient analysis offers interesting velocity overshoot effects, as shown in Fig. 4. As time progresses, the drift velocity response oscillates and the amplitude decreases for the structure having a thick spacer layer. For d = 20 nm, the velocity responses at two fields values, *i.e.*, 500 V/cm (solid line) and 1 kV/cm (dashed line), are shown in Fig. 4. It can be seen from the figure that the time needed to reach the velocity maximum (the time needed to charge up each particle) decreases with increases in the applied field.

These overshoot characteristics are understood as follows. Under the condition where the ionized impurity scattering is very small, the dominant scattering mechanism is polar optical phonon emission. When the initial thermal energy is smaller than optical phonon energy $\hbar\omega_0$ (35.4 meV), the electrons cannot emit polar optical phonons. This condition is easily satisfied at low lattice temperatures. After their energies reach $\hbar\omega_0$ by gaining energy from the field, they lose momentum and energy, and approach the steady state. Due to emission process threshold, ballistic transport behaviors are observable in the thick spacer structures.

The initial thermal energy is given to each electron using a random number while taking into account the two-dimensional density of states. It is considered that the average thermal energy for Q2DEG ($k_B T_l$) is smaller than that for the bulk mode (3/2 $k_B T_l$). Therefore, the conditions that cause the above ballistic phenomenon are easily realized in Q2DEG under low lattice temperatures.

Figure 6 shows calculated electric field distributions along the heterointerface under the gate using a macroscopic device simulator[14]. Through the macroscopic device modeling, we have obtained the conclusion that high values of low field mobility as well as large saturation velocities are very important to realize high speed operation. The present study concludes that high values of low field mobility can be expected in the Q2DEG due to the remote impurity scattering reduction. Moreover, the electric field under the gate is always very small, especially near the source, as shown in Fig. 6. Accordingly, additional velocity overshoot effects (corresponding to the ballistic transport phenomenon) which are also advantageous for the high speed operation, are expected.

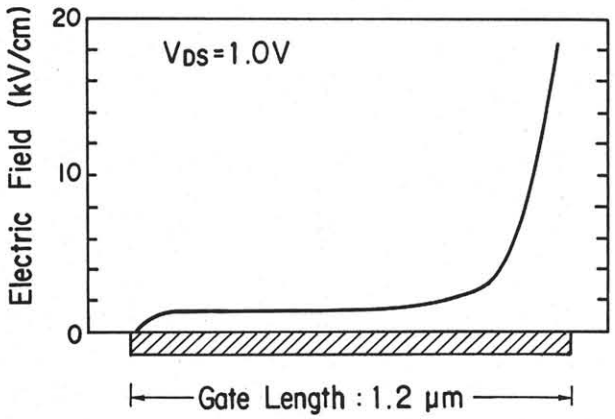

Fig. 6 Electrical field distributions along heterointerface 3 nm from the interface.

IV. CONCLUSION

The drift velocity responses peculiar to Q2DEG are discussed in detail based upon accurate physics. It is demonstrated that the remote ionized impurity scattering rate is reduced by increasing the thickness of the spacer layer. For the structures with a thick spacer layer, ballistic transport characteristics are observed at a lattice temperature of 77 K. Since the ionized impurity scattering rate is suppressed for these structures having a thick spacer layer, the most dominant scattering mechanism is polar optical phonon emission. However, the electrons do not have sufficient energy at low lattice temperature to emit polar optical phonons (~35.4 meV). Therefore, the electrons gain energy from the applied field without undergoing polar optical phonon emission. Accordingly, ballistic transport, which is advantageous phenomenon for realizing high speed operation, is expected. On the contrary, the electrons suffer ionized impurity scattering (mainly remote effect) when the spacer is thin. Hence, electron distribution is randomized, and the velocity overshoot effect corresponding to the ballistic transport phenomenon is weakened or eliminated.

ACKNOWLEDGMENTS

The authors thank Professors Hiroyuki Sakaki and Karl Hess for their valuable discussions. Thanks are also due to Takayoshi Nakashima for his encouragement.

REFERENCES

[1] T. Mimura, S. Hiyamizu, T. Fujii, and K. Nanbu, Jpn. J. Appl. Phys. **19**, L225 (1980).

[2] R. Dingle, H. L. Störmer, A. C. Gossard, and W. Wiegmann, Appl. Phys. Lett. **33** 665 (1978).

[3] S. Kawaji, J. Phys. Soc. Jpn. **27** 906 (1969).

[4] K. Hess, Appl. Phys. Lett. **35** 485 (1979).

[5] P. J. Price, Ann. Phys. **133** 217 (1981).

[6] S. Mori and T. Ando, Phys. Rev. B **19** 6433 (1979).

[7] J. Lee, H. N. Spector, and V. K. Arora, J. Appl. Phys. **54** 6995 (1983).

[8] W. Walukiewicz, H. E. Ruda, J. Lagowski, and H. C. Gatos, Phys. Rev. B **30** 4571 (1984).

[9] K. Yokoyama and K. Hess, Phys. Rev. B **33** 5595 (1986).

[10] K. Yokoyama and K. Hess, J. Appl. Phys., **59** 3798 (1986).

[11] W. Fawcett, A. D. Boardman, and S. Swain, J. Phys. Chem. Solids **31** 1963 (1970).

[12] T. Ando, J. Phys. Soc. Japan, **51** 3900 (1982).

[13] K. Hirakawa, H. Sakaki, and J. Yoshino, Appl. Phys. Lett., **45** 253 (1984).

[14] K. Yokoyama, M. Tomizawa, and A. Yoshii, Trans. IECE Japan, **J67-C** 810 (1984) (in Japanese).